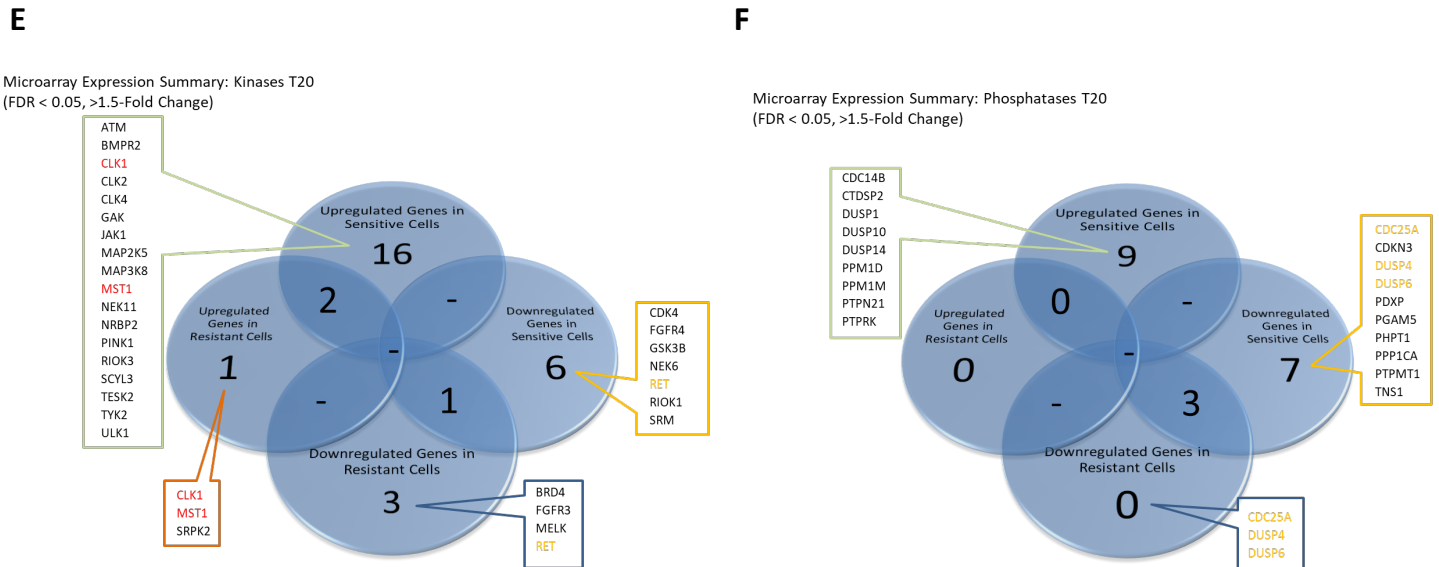
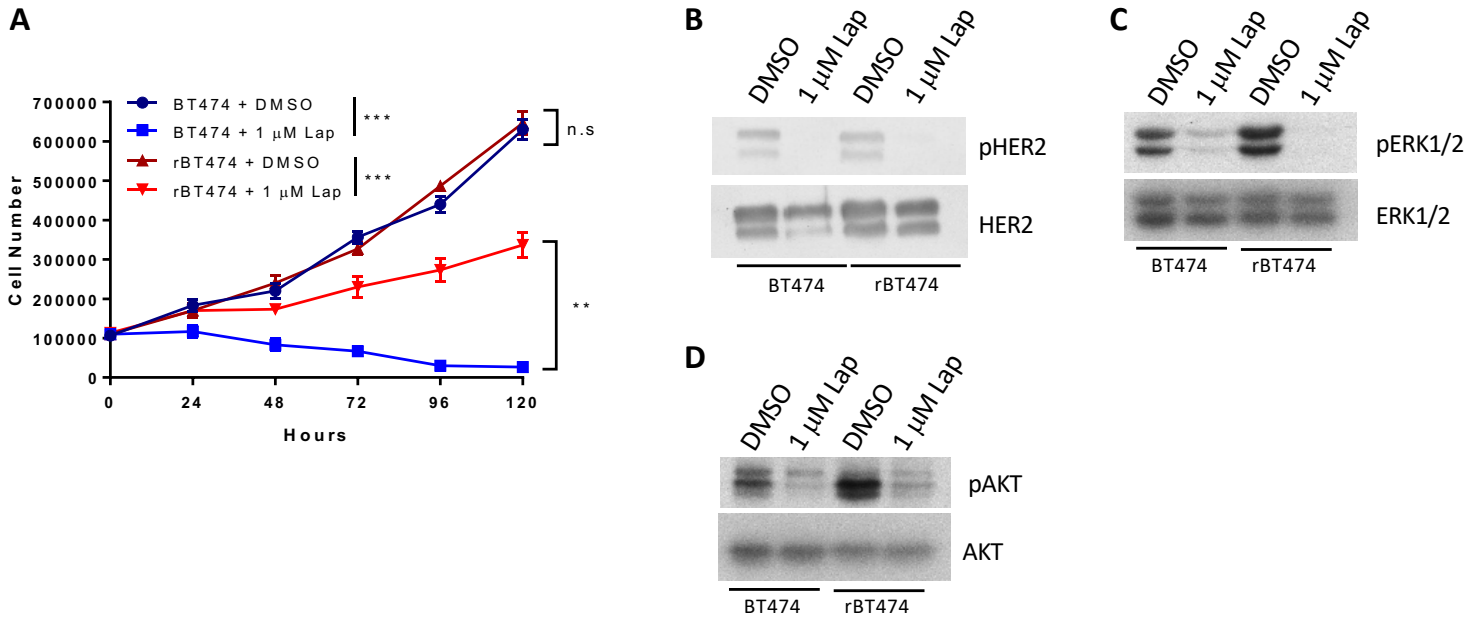


Cell Reports, Volume 29

Supplemental Information

**CD36-Mediated Metabolic Rewiring
of Breast Cancer Cells Promotes
Resistance to HER2-Targeted Therapies**

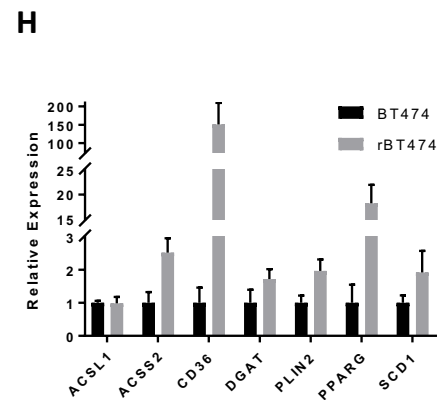
William W. Feng, Owen Wilkins, Scott Bang, Matthew Ung, Jiaqi Li, Jennifer An, Carmen del Genio, Kaleigh Canfield, James DiRenzo, Wendy Wells, Arti Gaur, R. Brooks Robey, Jessie Yanxiang Guo, Ryan L. Powles, Christos Sotiriou, Lajos Pusztai, Maria Febbraio, Chao Cheng, William B. Kinlaw, and Manabu Kurokawa



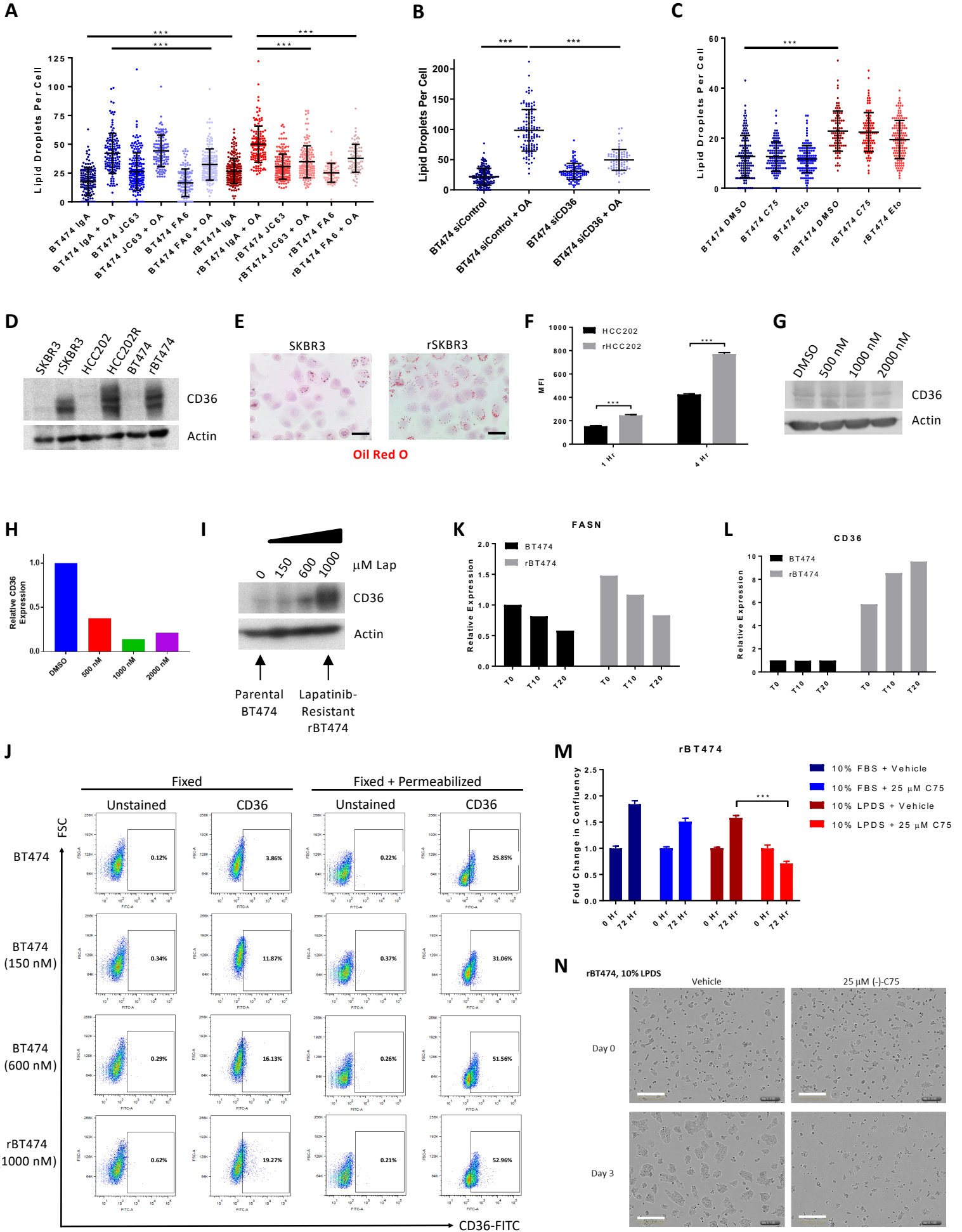
G

Top 20 Upregulated GO Biological Process Terms at Baseline

Gene Set Name	# Genes	Enrichment Score	FDR q-value
GO_IMMUNE_SYSTEM_PROCESS	30	4.34	4.68E-08
GO_TISSUE_DEVELOPMENT	26	4.91	4.68E-08
GO_POSITIVE_REGULATION_OF_DEVELOPMENTAL_PROCESS	22	5.54	1.42E-07
GO_EPITHELIUM_DEVELOPMENT	20	6.09	1.60E-07
GO_REGULATION_OF_CELL_DIFFERENTIATION	24	4.62	4.22E-07
GO_CELLULAR_RESPONSE_TO_ORGANIC_SUBSTANCE	26	4.05	1.04E-06
GO_NEGATIVE_REGULATION_OF_RESPONSE_TO_STIMULUS	22	4.65	1.55E-06
GO_NEGATIVE_REGULATION_OF_MULTI_ORGANISM_PROCESS	9	17.12	1.92E-06
GO_POSITIVE_REGULATION_OF_CELL_DIFFERENTIATION	17	5.95	2.66E-06
GO_NEGATIVE_REGULATION_OF_CELL_COMMUNICATION	20	4.83	3.13E-06
GO_RESPONSE_TO_ENDOGENOUS_STIMULUS	22	4.37	3.13E-06
GO_POSITIVE_REGULATION_OF_MULTICELLULAR_ORGANISMAL_PROCESS	21	4.34	7.16E-06
GO_REGULATION_OF_MULTICELLULAR_ORGANISMAL_DEVELOPMENT	23	3.96	7.16E-06
GO_CELLULAR_LIPID_METABOLIC_PROCESS	17	5.34	7.77E-06
GO_INNATE_IMMUNE_RESPONSE	14	6.49	1.26E-05
GO_IMMUNE_RESPONSE	18	4.71	1.70E-05
GO_REGULATION_OF_CELL_PROLIFERATION	21	4.02	1.70E-05
GO_REGULATION_OF_TRANSPORT	23	3.65	2.04E-05
GO_ION_TRANSPORT	19	4.34	2.33E-05
GO_LIPID_METABOLIC_PROCESS	18	4.45	3.09E-05



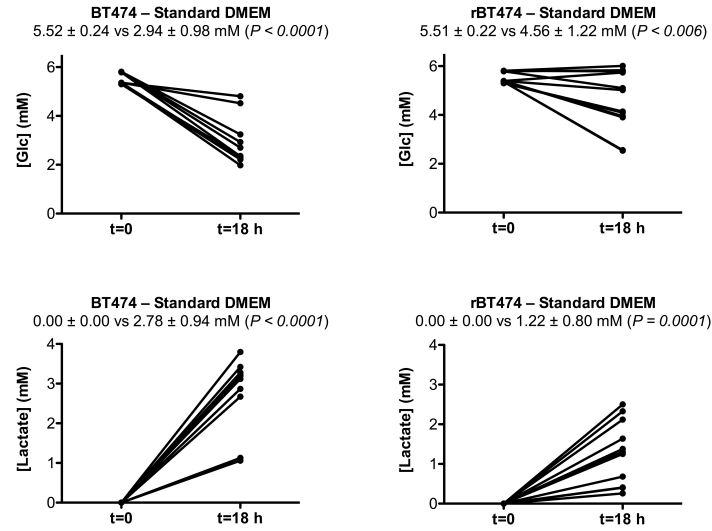
Supplemental Figure S1. Related to Figure 1. (A) Proliferation of BT474 and rBT474 cells was measured by cell counting 0, 24, 48, 72, 96, and 120 hours after treatment with 1 μ M lapatinib (Mean +/- SD from n = 2 experiments). Significance assessed by non-paired Student's t-test with significance set at ** p<0.005, *** p<0.0005. **(B-D)** BT474 and rBT474 cells treated with lapatinib for 24 hours and assessed for pHER2 (B), pAKT (C), and pERK1/2 (D) levels. **(E-F)** Venn diagram of all kinases (E) and phosphatases (F) that exhibit a 1.5-fold or greater change 20 hours after 1 μ M lapatinib treatment as compared to untreated controls (FDR < 0.05). Red text signifies genes upregulated in both resistant and sensitive cells. Orange text signifies genes downregulated in both resistant and sensitive cells. **(G)** Top 20 Gene Ontology (GO) terms upregulated in rBT474 as compared to parental BT474 cells at baseline (T0). Bolded and italicized rows denote terms directly related with lipid metabolism. **(H)** RT-qPCR validation of genes related to lipid metabolism found to be upregulated in rBT474 cells by microarray analysis (Mean +/- SEM from n = 3 experiments).



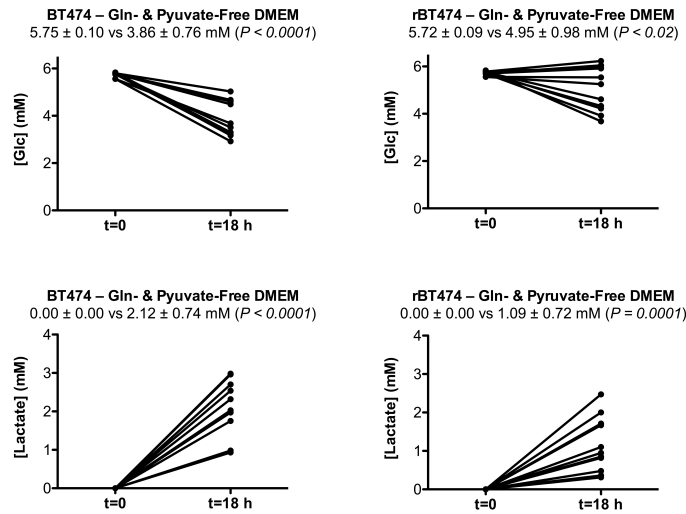
Supplemental Figure S2. Related to Figure 2. **(A)** BT474 and rBT474 cells were treated with 20 $\mu\text{g}/\text{mL}$ control IgA or JC63.1 anti-CD36 function blocking antibodies for 2 hours and were then cultured in the presence or absence of 100 μM oleic acid (OA) for additional 8 hours. Accumulation of lipid droplets was analyzed by Oil Red O staining and was quantified by counting 100-200 cells (Mean \pm SD from $n = 3$ experiments). **(B)** BT474 and rBT474 cells were transfected with siControl or siCD36 siRNA as in Figure 4A. Cells were cultured in the presence or absence of 100 μM OA for 8 hours. Accumulation of lipid droplets was analyzed by Oil Red O staining and was quantified by counting 100-200 cells (Mean \pm SD from $n = 3$ experiments). **(C)** BT474 and rBT474 cells were treated with 50 μM (-)-C75 or 100 μM etomoxir (Eto) for 10 hours. Accumulation of lipid droplets was analyzed by Oil Red O staining and was quantified by counting 100-200 cells (Mean \pm SD from $n = 3$ experiments). (A-C) Significance assessed by non-paired Student's t-test with significance set at *** $p < 0.0001$. **(D)** CD36 expression of lapatinib resistant SKBR3, HCC202, and BT474 cells (rSKBR3, rHCC202, and rBT474, respectively) as compared to lapatinib sensitive parental cells **(E)** Representative image of SKBR3 and rSKBR3 cells stained with Oil Red O from $n = 3$ experiments. Scale bar indicates 20 μm **(F)** HCC202 and rHCC202 cells were cultured in the presence of 2 μM BODIPY FL C16 for the indicated periods of time. Median fluorescence intensity (MFI) was measured by flow cytometry. Depicted is the mean MFI of three replicate samples per time point \pm SD from one representative experiment out of $n = 3$ experiments. Significance assessed by non-paired Student's t-test with significance set at *** $p < 0.0005$. **(G-H)** BT474 cells were treated with 500 nM, 1000 nM, or 2000 nM lapatinib for 8 days to intentionally select for surviving inherently drug tolerant cells. These cells were assessed for CD36 expression by western blot (G) and RT-qPCR (H). **(I-J)** rBT474 were generated over the span of several months by gradually increasing in lapatinib concentrations in the tissue culture media. CD36 expression was measured by western blot (I) and flow cytometry (J) at various timepoints. **(K-L)** BT474 and rBT474 were harvested 0 (T0), 10 (T10), and 20 hours (T20) after

treatment with 1 μ M lapatinib (n = 4 per treatment). Gene expression of FASN (K) and CD36 (L) of BT474 and rBT474 cells measured by microarray. **(M-N)** rBT474 cells were treated with 25 μ M (-)-C75 in media containing 10% FBS or 10% Lipoprotein-Depleted Serum (LPDS). Cell proliferation was measured by live cell imaging using an Incucyte Zoom imager 72 hrs after drug treatment. Results depict average change in confluency from 3 replicate wells +/- SD from n = 3 experiments (M). Representative images shown in (N). Scale bar indicates 100 μ m. Significance assessed by non-paired Student's t-test with significance set at *** p<0.0001.

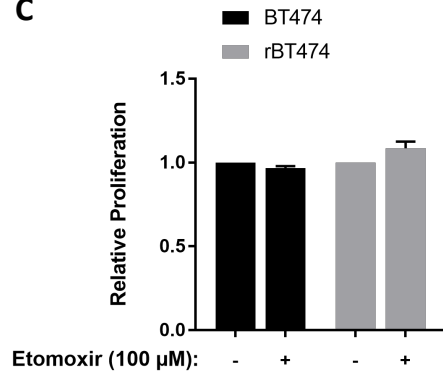
A



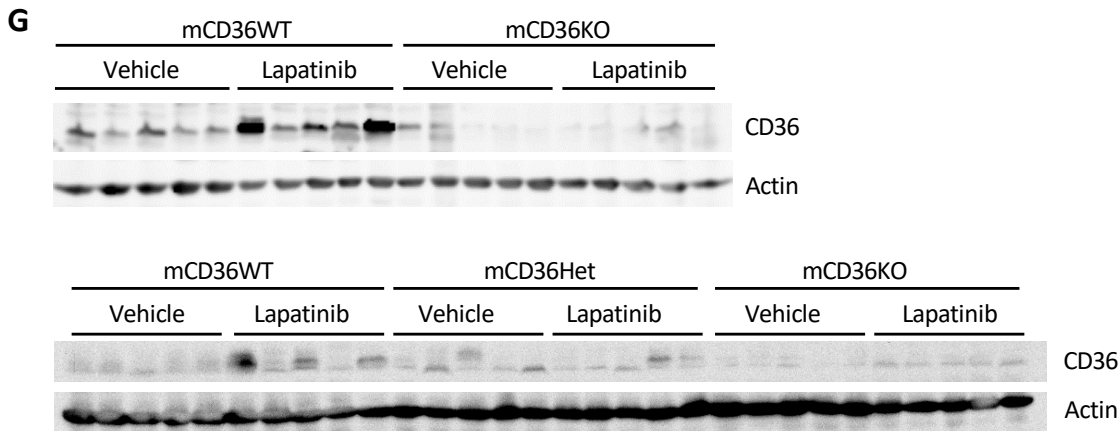
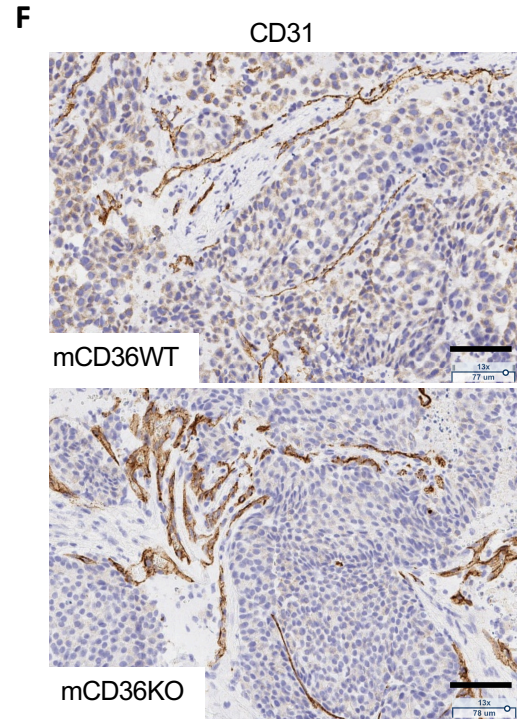
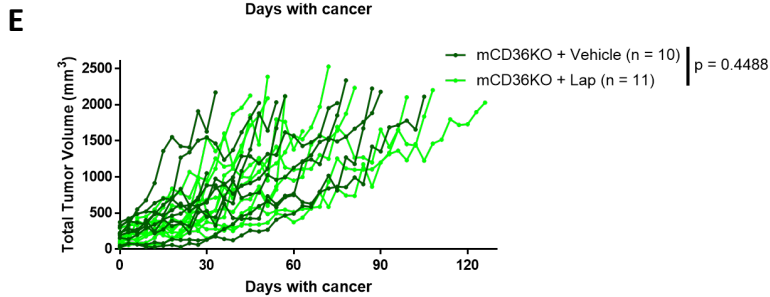
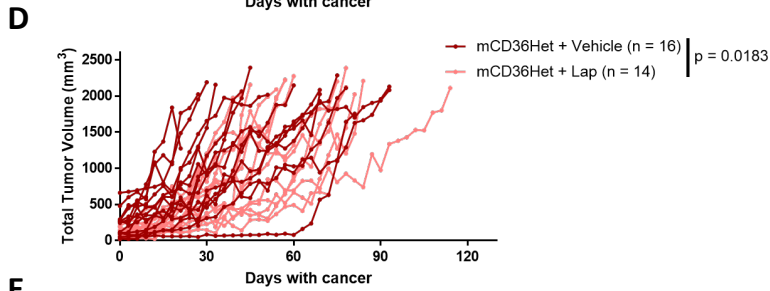
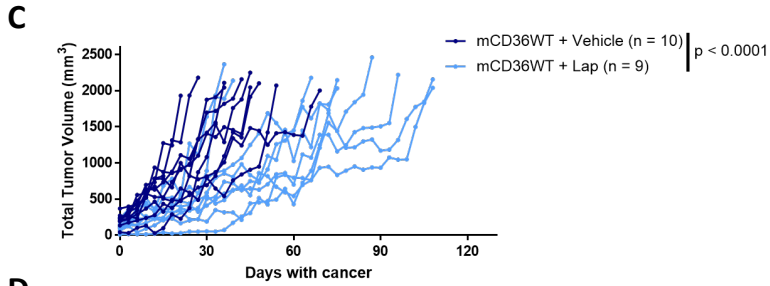
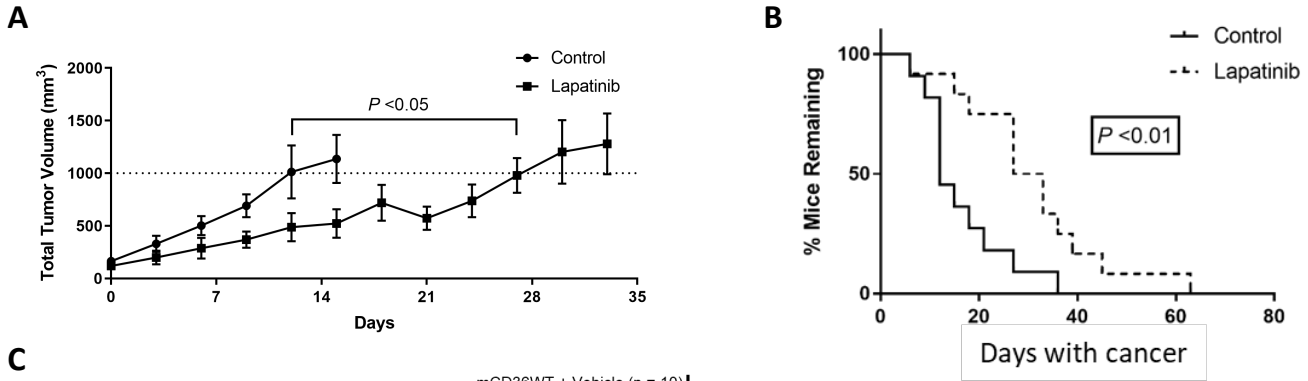
B



C



Supplemental Figure S3. Related to Figure 3. (A-B) Net glucose disappearance and lactate accumulation were monitored in basal 5.6 mM glucose-containing media over 18 hours in both the presence (A) and absence (B) of 2 mM glutamine and 1 mM pyruvate as alternate metabolic substrates. The observed rate of glucose disappearance was uniformly linear over this period (data not shown) and, because it was non-exhaustive, was ostensibly non-limiting for lactate accumulation under these conditions. These data normalized for both cellular protein content and overlying culture medium volume were used to generate Figure 3B. Statistical significance assessed by paired Student's *t*-testing. **(C)** Proliferation rates, assayed by MTS reduction over 48 hours as described previously (Canfield et al., 2015), did not differ between BT474 and rBT474 cells cultured in media containing 5.6 mM glucose, 2 mM glutamine, and 1 mM pyruvate in either the presence or absence of 100 μ M etomoxir, suggesting that differences in metabolism under these conditions cannot be explained by differences in cell proliferation (Mean +/- SEM from n = 3 experiments).

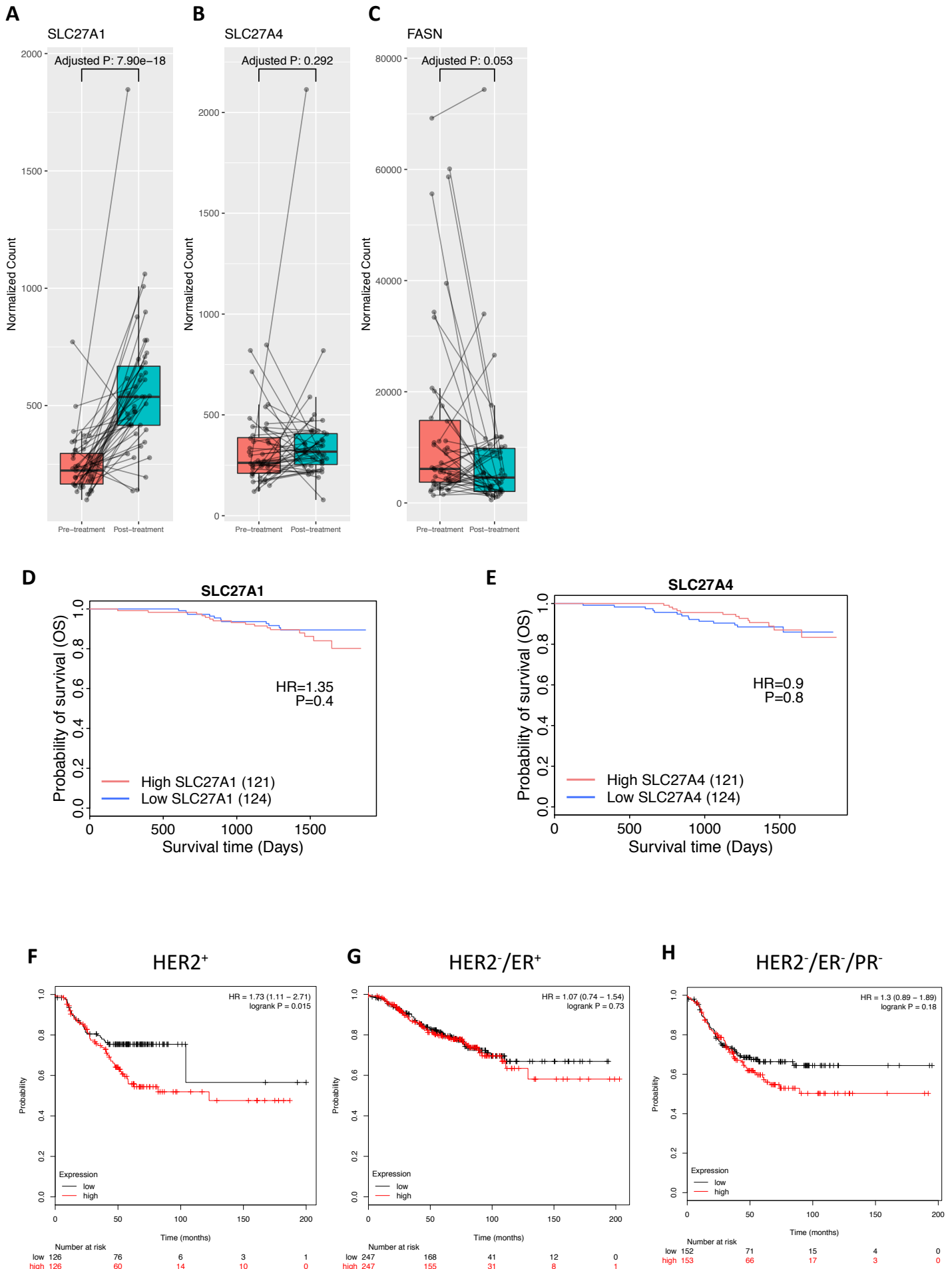


H

		Vehicle				Lapatinib			
		- Met	+ Met*	Total	% With Met	- Met	+ Met*	Total	% With Met
CD36	+/+	8	2	10	20.00%	2	6 (1)	9	77.78%
	+/F	8	8	16	50.00%	12	1 (1)	14	14.29%
	F/F	7	3	10	30.00%	8	3	11	27.27%

*The total numbers of mice exhibiting lung metastases (Met) are reported and number of mice exhibiting metastatic tumors in other sites (such as liver and small intestine) are noted in parentheses.

Supplemental Figure S4. Related to Figure 5. (A-B) Daily treatment with 100 mg/kg lapatinib BID suppresses tumor growth of *MMTV-neu* mice (A) and prolongs survival (B). Significance assessed by log-rank test * $P < 0.05$ (Mean \pm SEM for 10-11 mice). **(C-E)** Individual growth curves depicting total tumor volume over time for mCD36WT (C), mCD36Het (D), and mCD36KO (E) mice treated with vehicle or lapatinib. **(F)** Representative images of CD31 stained mCD36WT and mCD36KO tumors. Scale bar indicates 77 μm . **(G)** Western blot analysis of mCD36WT and mCD36KO tumors collected from $n = 5$ mice per group from Figure 5F-H. **(H)** Incidence of metastasis from the mice in Figure 5F-H. The majority of metastases were observed in the lungs but the numbers inside the parentheses note the presence of metastases observed in other sites, such as liver or small intestine.



Supplemental Figure S5. Related to Figure 6. (A-C) SLC27A1 (A), SLC24A4 (B), and FASN (C) expression was measured by RNA sequencing in 44 pairs of tumor biopsies pre- and post-treatment with HER2-targeted therapy. **(D-E)** Overall survival of 245 patients with pre-treatment biopsies from the NeoALLTO trial stratified by SLC27A1 (D) and SLC27A4 (E) expression. **(F-H)** TCGA Subtype-specific Kaplan Meier plots were plotted using the Kaplan-Meier plotter webtool (Lánczky et al., 2016) (<http://kmplot.com/analysis/>). **(F)** Relapse free survival of TCGA HER2-positive breast cancer patients dichotomized by CD36 microarray expression. **(G)** Relapse free survival of TCGA HER2-negative ER-positive breast cancer patients dichotomized by CD36 microarray expression. **(H)** Relapse free survival of TCGA triple-negative breast cancer patients dichotomized by CD36 microarray expression.